Appl Magn Reson (2018) 49:335–344
https://doi.org/10.1007/s00723-017-0973-y

Applied Magnetic Resonance

ORIGINAL PAPER

A Variable Temperature X- and W-Band EPR Study of Fe-Doped SiCN Ceramics Annealed at 1000, 1100, and 1285 °C: Dangling Bonds, Ferromagnetism and Superparamagnetism

S. I. Andronenko[1] · **A. A. Rodionov**[1] · **S. K. Misra**[2]

Received: 22 July 2017 / Revised: 14 December 2017 / Published online: 1 February 2018

Abstract Polymer-derived SiCN ceramics, annealed (also referred to as pyrolyzed) at 1000, 1100, and 1285 °C, and doped with Fe(III) acetylacetonate, are investigated by electron paramagnetic resonance (EPR) from 4 to 120 K at X-band (9.425 GHz). In addition, the SiCN ceramic, annealed at 1100 °C, was studied by EPR at 300 K at W-band (93.96 GHz). There was observed a significant increase in EPR linewidth due to dangling bonds ($g = 2.001$) below 20 K at X-band. The low-field X-band FMR line ($g \approx 12$) indicated the presence of ferromagnetic Fe_5Si_3 crystallites. There were found two EPR lines due to carbon-related dangling bonds: (1) those present as defects on the surface of the free-carbon phase (as sp^2 carbon-related dangling bonds with $g = 2.0011$) and (2) those present within the bulk of carbon phase (as sp^3 carbon-related dangling bonds with $g = 2.0033$). On the other hand, the intense low-field EPR signal observed at X-band was not observed at W-band. As well, there was observed splitting of the single broad EPR signal observed at $g = 2.05$ at X-band into two signals at W-band at $g = 1.99$ and $g = 2.06$, due to two different Fe-containing superparamagnetic nanocrystallites. Two new EPR signals, not observed at X-band, were observed at W-band, namely at $g = 2.28$ and $g = 3.00$, which are also due to $g_{\|}$ of these superparamagnetic nanocrystallites.

✉ S. I. Andronenko
sergey.andronenko@gmail.com

[1] Institute of Physics, Kazan Federal University, Ul. Kremlevskaya, 18, Kazan 420008, Russian Federation

[2] Department of Physics, Concordia University, 1455 de Maisonneuve Boulevard West, Montreal, QC H3G 1M8, Canada

1 Introduction

A new ceramic material, polymer-derived silicon carbonitride (SiCN), has recently been exploited for microelectromechanical systems (MEMS) applications [1]. Simple and effective manufacturing technologies for this material have been developed using liquid-polymer precursor technique [2, 3]. SiCN ceramics, derived from liquid polysilazane precursor, possess many outstanding physical properties, such as hardness, fracture strength, creep resistance and high functional temperature. Fe-doped SiCN ceramics, referred to hereafter as SiCN/Fe, can be easily produced by the addition of various iron-containing compounds to the polymer precursor. Recent reviews of synthesis and characterization of polymer-derived SiCN/Fe ceramics were presented by Zaheer et al. [4], Hojamberdiev et al. [5], and Mera et al. [6]. SiCN ceramics annealed (the term pyrolyzed is also used instead of annealing) above 1000 °C have excellent thermal/mechanical and magnetic properties for high-temperature and high-pressure applications; in particular, for magnetic and pressure sensors [7–10]. Electron paramagnetic resonance (EPR), which is a very sensitive technique to probe environments around a paramagnetic center, enables one to distinguish between different sources of magnetism produced by Fe-containing crystallites.

SiCN ceramic is a wide-band semiconductor with the energy gap $\sim$ 3.8 eV [11]. Its conductivity varies widely depending on annealing temperature and the impurities [12, 13] present. Different kinds of defects, which can serve as donors or acceptors, influence electrical conductivity, and therefore the EPR investigations of the defects can help to understand the mechanism of conductivity in such compounds.

The EPR technique has been successfully used to investigate pure SiCN ceramic samples [7, 14–17], as well as SiBCN ceramics [18]. Recently, Li et al. [19] reported EPR spectra of sp^2- and sp^3-dangling bonds in SiCON ceramics. In particular, a detailed investigation of dangling bonds in these ceramics has been carried out by EPR at several frequencies from 9.5 GHz to as high as 170 GHz at various temperatures from 4 to 300 K [7]. There was observed an intense EPR line due to carbon related sp^2-dangling bonds, located on the surface of free-carbon phases with $g = 2.0027$. In the synthesis, these dangling bonds are first formed during ceramization, thereafter C–H bonds are broken, allowing for the formation of free-carbon phase [20]. Recent confirmation of such origin of EPR signal due to dangling bonds was obtained by Tomasella et al. [21, 22]. Kobayashi et al. [23] reported observation of an EPR signal in UV-irradiated SiCN films, associated with nitrogen-related dangling bonds. Savchenko et al. [24] investigated SiCN films and found three EPR signals, that with $g = 2.0033$ due to sp^2 carbon-related dangling bonds, with $g = 2.009$, attributed to the interface defect representing threefold-coordinated Si dangling bond, and with $g = 2.05$, attributed to the trapped holes on Si atoms.

The purpose of this paper is to present an analysis of new X- and W-band EPR data to understand better the local magnetic structure of SiCN/Fe ceramic composites and the influence of annealing temperature on its magnetic properties,

and in particular, to identify the Fe-containing crystallites, which determine the magnetic properties of these doped SiCN/Fe ceramics. An important aim of this work is to develop a better understanding of the carbon-related dangling bonds present in the SiCN ceramics samples, doped with Fe ions.

2 Experimental Results

2.1 Synthesis

The synthesis of SiCN ceramics, doped with Fe ions, used in the present investigations, has been described elsewhere [7, 8].

2.2 X-Band EPR Spectra

X-band (9.425 GHz) EPR spectra were recorded on a Bruker ESP300 spectrometer in the temperature range of 4.2–120 K, using an Oxford gas flow cryostat. There were found at least two different sources of magnetism, as exhibited by two different EPR lines, whose temperature behaviors are different from each other.

The EPR spectra are shown in Fig. 1a–c for the SiCN/Fe samples annealed at 1000, 1100 and 1285 °C. The narrow EPR signals are due to dangling bonds. They are shown in Fig. 1d. The variation of the corresponding EPR linewidth is shown in the temperature range 4.2–120 K in Fig. 2.

2.3 FMR Line

An inspection of Fig. 1a–c reveals the presence of a distinct FMR line (A) situated at about 200–400 G with a peak-to-peak width of $\sim$ 600 G. As well, it shows a structure on the lower magnetic field side, which enhances with decreasing temperature. This line is due to the ferromagnetic particles of Fe_5Si_3 with $T_C = 393$ K [25] present in the sample, as identified in [8] from temperature dependence of the linewidth. There is also observed a broad line near $g = 2.05$, referred to hereafter as line B, whose intensity and linewidth do not change in the temperature range under investigation from 4.2 to 120 K. The shape of this line is very similar to that calculated by Kliava et al. [26] for an assembly of superparamagnetic particles, randomly dispersed in a diamagnetic host material. Therefore, this line is assigned to Fe-containing superparamagnetic particles. There is observed a considerable decrease of the integrated intensity of the X-band FMR line (A) below 250 K with decreasing temperature for all three SiCN/Fe samples, annealed at 1000, 1100, 1285 °C, investigated here. However, this line was detected only partly and this fact prevents detailed analysis of its linewidth and double-integrated intensity.

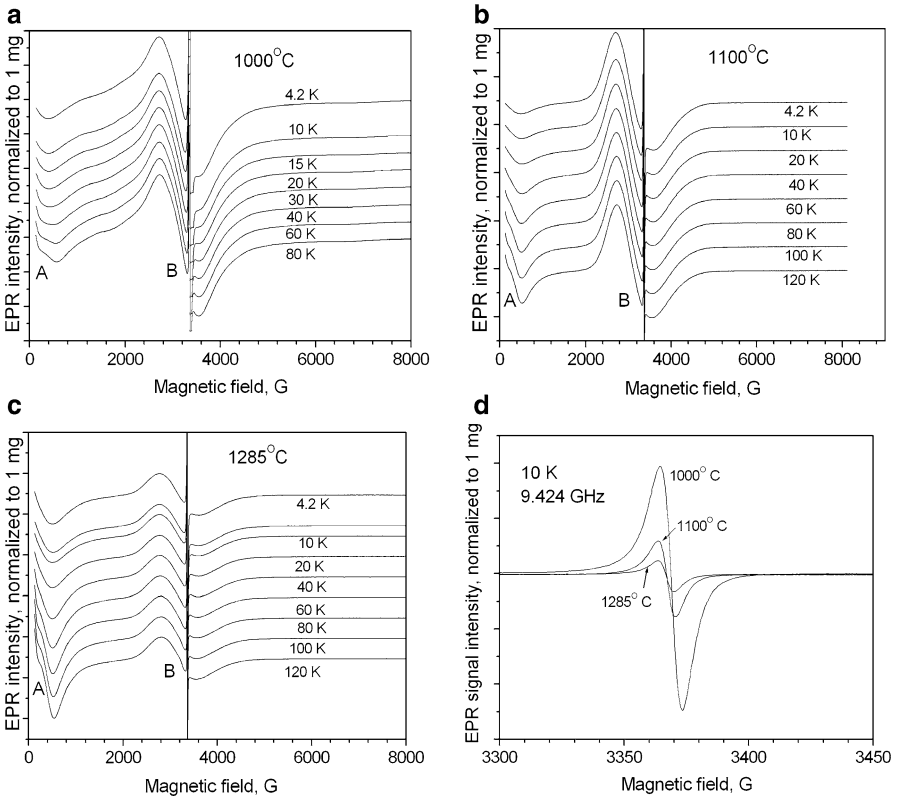

Fig. 1 Variation of the first-derivative X-band EPR spectrum with temperature for the SiCN/Fe ceramic samples annealed at **a** 1000 °C, **b** 1100 °C, **c** 1285 °C, **d** the EPR lines due to carbon dangling bonds for the SiCN/Fe ceramic samples annealed at 1000, 1100 and 1285 °C at 10 K

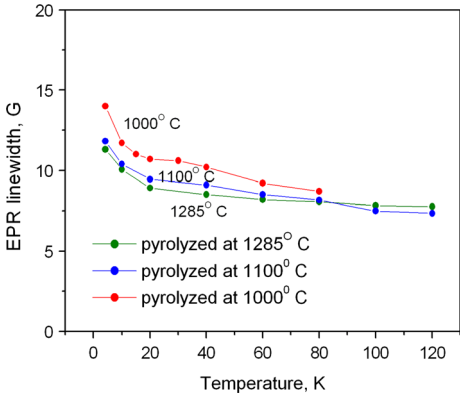

Fig. 2 Temperature dependence of the X-band EPR linewidth of carbon-related dangling bonds for the SiCN/Fe ceramic samples annealed at 1000, 1100 and 1285 °C

2.4 EPR Line Due to Dangling Bonds

The sharp, narrow line with Lorentzian lineshape at $g = 2.001$ was observed in all SiCN/Fe samples investigated here, as shown in Fig. 1d. It is due to dangling bonds. Its EPR linewidth, i.e., 5.4 G at 300 K for the SiCN sample annealed at 1100 °C was found to be larger than those in the pure SiCN ceramic samples, e.g., 1.2 G in pure SiCN samples annealed at 1100 °C [7]. This is because there is an additional contribution to the EPR linewidth due to the dipole–dipole interactions between carbon-related dangling bonds and Fe ions in the doped SiCN/Fe sample as compared to that in the pure SiCN sample.

2.4.1 g Values of EPR Lines Due to Carbon-Related Dangling Bonds

At room temperature, the EPR line, assigned to the carbon-related dangling bonds exhibits the value: $g = 2.001 \pm 0.001$, different from that in a pure SiCN ceramics ($g = 2.0027$) [7]. The experimentally obtained g value reveals unequivocally that the observed EPR signal in these samples is due to carbon-related defects [27, 28], rather than that due to silicon-related dangling bonds, which is characterized by the g value of 2.0055 [28].

2.4.2 Temperature Dependences of the EPR Linewidth

The EPR linewidth associated with carbon-related dangling bonds is strongly temperature dependent as shown in Fig. 2. The temperature dependence of this line is very similar to that in pure SiCN ceramics without doping [7]. However, the EPR linewidth in this sample is considerably larger due to additional dipole–dipole and exchange interactions among dangling bonds and Fe-containing nanograins. This temperature dependence can be explained to be due to the influence of the exchange interaction between spins of carbon-related dangling bonds [29], similar to that in pure SiCN samples [7]. The exchange interaction was responsible in pure SiCN ceramic sample annealed at 1200 °C to effect a considerable exchange narrowing, which led to an extremely small EPR linewidth of $\Delta B_{pp} = 0.7$ G. It is noted that another analysis of temperature dependence of linewidth due to carbon-related dangling bonds in α-SiC: H films was provided in [30]. The decrease of EPR linewidth was there explained to be due to thermally activated jumps, which become more intense with increasing temperature, thus averaging the effective local magnetic fields, which results in a decrease of the EPR linewidth.

3 W-Band EPR Spectrum

3.1 Fe-Containing Crystallites

W-band EPR study of the SiCN/Fe ceramic sample, annealed at 1100 °C was carried out at 300 K at 93.96 GHz on an Elexsys-680 EPR spectrometer at the Federal Center of Shared Facilities of Kazan Federal University. This EPR spectrum

is assembled from five subsequent EPR spectra recorded in the ranges: 500–8500; 8000–18,500; 18,000–28,500; 28,000–38,500; and 38,000–48,000 G. It is shown in Fig. 3a. For comparison, the EPR spectrum of *sp*-dangling bonds in the same sample is shown in Fig. 3b.

As seen from Fig. 3a, there was observed splitting of X-band EPR signals due to enhanced resolution at the higher frequency of W-band. The broad EPR signal at $g \sim 2.05$ at X-band splits into two EPR signals at $g = 2.06$ and $g = 1.99$, at W-band. The origin of these two lines has been discussed in [8], establishing that they are due to Fe-containing particles. There appear two additional lines at W-band at $g = 3.0$ and $g = 2.28$ (Fig. 3a).

The interpretation of the EPR spectra with $S = 1/2$ in anisotropic polycrystalline samples were described in details in [31], and the shape of the EPR signals with $g = 3.0$ and $g = 2.28$ observed here is consistent with the analysis presented in [31].

The Fe-containing nanocrystallites are superparamagnetic species with enhanced magnetic moments, which are highly anisotropic. The spin Hamiltonian used for simulation of EPR spectrum of these nanocrystallites with an effective spin $S = 1/2$ is expressed as follows:

$$H = \mu_B[g_{||}B_zS_z + g_{\perp}(B_xS_x + B_yS_y)], \quad (1)$$

where μ_B is the Bohr magneton; g_x, g_y, g_z are the components of the g matrix, and B_z, B_x, B_y are the magnetic field components.

The simulated W-band EPR spectrum due to two different Fe(III) containing polycrystallites based on the spin Hamiltonian, given by Eq. 1, is an overlap of two EPR signals, S1: characterized by $g_{\perp} = 2.045$ and $g_{||} = 3.10$, and S2: characterized by $g_{\perp} = 1.99$, $g_{||} = 2.28$. It is shown in Fig. 4a. The best-fit spin Hamiltonian (SH) parameters to reproduce the observed W-band and X-band EPR spectra are listed in Table 1. The simulated X-band spectrum is shown in Fig. 4b.

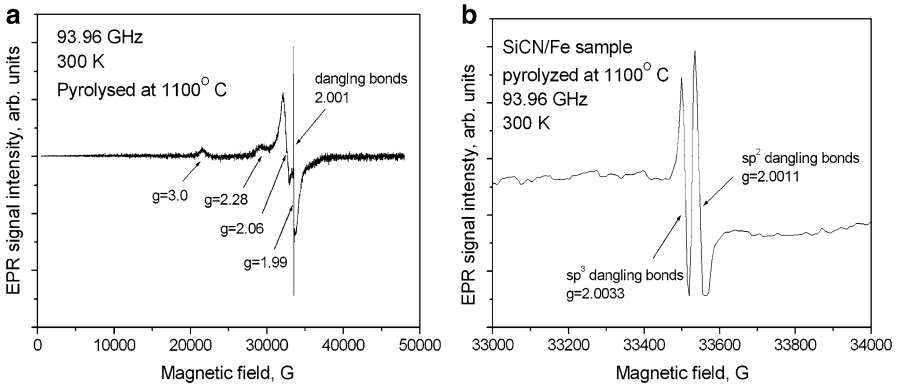

Fig. 3 **a** W-band EPR/FMR spectrum of SiCN/Fe ceramic annealed at 1100 °C at 93.96 GHz at 300 K. **b** The central part of the W-band spectrum with well-resolved carbon-related dangling bond EPR signals in the SiCN/Fe sample annealed at 1100 °C

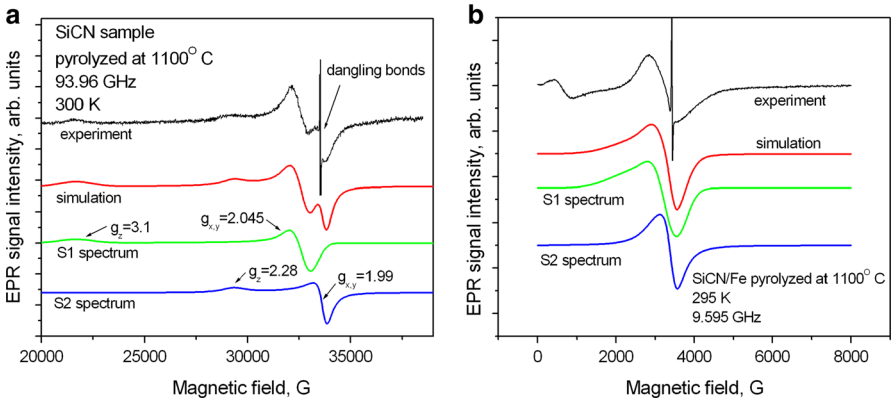

Fig. 4 **a** Simulation of the EPR spectrum (red) recorded at 94 GHz at 300 K in the SiCN/Fe sample annealed at 1100 °C. The experimental spectrum is in black. The EPR lines belonging to dangling bonds, indicated by arrow. **b** Simulation of the EPR spectrum (red) recorded at 9.6 GHz in the same sample, as an overlap of S1 and S2 components as described in the text (color figure online)

Table 1 The spin Hamiltonian parameters as determined from W-band and X-band EPR spectra in the SiCN/Fe ceramic sample annealed at 1100 °C

EPR signal (lineshape)	$g_x = g_y$	g_z	$\Delta B_{ppx} = \Delta B_{ppy}$ (G)		ΔB_{ppz} (G)		Relative intensity
			W-band	X-band	W-band	X-band	
S1 (Gauss)	2.045	3.10	900	600	1600	1200	0.5
S2 (Lorentz)	1.990	2.29	460	320	800	600	0.5

The W-band EPR spectrum did not show any EPR line in the low-field region, covered in Fig. 3a, in contrast to the X-band low-field EPR line A (Figs. 1a–c, 4b). This line is due to ferromagnetic nanocrystallites, thus its line position depends on internal exchange and dipole–dipole magnetic fields and for W-band it appears to be out of the range of the external magnetic field, and thus not observed at W-band. It is noted that the W-band signals with $g = 3.0$ ($H_{res} \approx 2270$ G) and $g = 2.28$ ($H_{res} = 2980$ G) are not clearly observed at X-band, as seen from Fig. 3b because of low resolution of g at the lower frequency of X-band. The simulations of X-band and W-band spectra were carried out with the same SH parameters, except for the linewidths ΔB_{ppx}, ΔB_{ppy}, ΔB_{ppz}, which are slightly larger at W-band as expected due to its higher frequency. The simulated X-band spectrum does not exhibit any signs of additional signals. They are very broad and hidden in the inhomogeneous EPR signal at $g = 2.05$. On the other hand, as expected, these EPR lines are well resolved at W-band.

However, it can be assumed that the line A in the X-band and the lines with $g = 3.0$ and $g = 2.28$ in W-band are connected with to ferromagnetic particles. A shift of the ferromagnetic resonance lines from the position of $g = 2$ is due to the internal local magnetic fields, the values of which probably are not changed with the

external magnetic fields. Therefore, the resonant fields are shifted from $g = 2$ to the same value in X- and W-bands. This shift turned out to be $\approx$ 3000 G for the line with $g = 2.28$ in W-band and for the line A in X-band. So, this explains absence of any line in low-field region at W-band.

3.2 EPR Lines Due to Carbon-Related Dangling Bonds

The two rather narrow W-band EPR lines with $g = 2.0011$ and $g = 2.0033$ (Fig. 3a) are due to carbon-related dangling bonds, amplified to show better resolution in Fig. 4b.

The dangling bonds are created due to the formation of incomplete "carbon-cage" structure by the free-carbon phase present in SiCN ceramics [32, 33], as proposed initially in the context of SiCO ceramics. Recent molecular-dynamics calculations suggest that the carbon ions are aromatically bonded and characterized by graphene network structure in SiCN ceramics [34], which connects SiCN nanocrystallites. This graphene network structure can be broken, producing sp^2-dangling bonds. Bulk carbon structure is formed in SiCN ceramics at annealing temperatures above 1100 °C [14–16, 20] and this structure can provide sp^3-dangling bonds. The origin of the EPR lines due to sp^2 and sp^3 carbon-related dangling bonds has been discussed in the literature [15, 17, 23, 35, 36], but there has been offered no unequivocal explanation as to whether it is due to sp^3 or sp^2 carbon-dangling bonds. The assignment of these two EPR lines can be made here, based on the similarity of their g values to those observed in ultradispersed diamond ($g = 2.0028$) and diamond heated to 1600 °C, which became converted to graphite-like system ($g = 2.0013$) [35, 36]. The EPR signal with $g = 2.0028$ is due to sp^3 carbon-related dangling bonds, whereas the signal with $g = 2.0013$ is due to sp^2 carbon-related dangling bonds. Furthermore, the coexistence of sp^2 and sp^3 carbon-related dangling bonds has been confirmed by X-ray photoelectron spectroscopy, as discussed by Li et al. [19] in polymer-derived SiCON ceramic. (It is polymer-derived compound, which is similar to SiCN, but possesses oxygen content.) They assigned the EPR signal at $g = 2.0012$ to sp^2 carbon-related dangling bonds. Accordingly, one can explain the occurrence of the two EPR line observed here at W-band as follows. The EPR line with $g = 2.0033$ is due to sp^3 carbon-related dangling bonds that exist in the amorphous carbon part of the sample, and the EPR line with $g = 2.0011$ is due to the sp^2 carbon-related dangling bonds, which are located in the broken aromatic rings of graphene layers in the sample.

The formation of bulk graphite-like structure occurs for annealing at temperatures above 1100 °C, and therefore the intensity of the EPR signal for sp^3-dangling bonds increased in this sample.

4 Concluding Remarks

The salient features of the present study are as follows:

1. The two observed EPR lines at $g = 2.0011$ and 2.0033, well resolved at the high-frequency W-band (94 GHz), are due to carbon-related dangling bonds: (a) those associated with the aromatic rings of graphene layers with the g value 2.0011 (sp^2); and (b) those existing in the bulk of "free" carbon phase with $g = 2.0033$ (sp^3).
2. The high-frequency W-band EPR data on the SiCN/Fe samples clearly shows that the central broad EPR line observed at X-band splits into two lines, due to the presence of two different superparamagnetic crystalline phases, with anisotropic magnetic moments, as deduced from the EPR lines at $g = 3.00$ and $g = 2.28$.

Acknowledgements This research was supported by the Natural Sciences and Engineering Research Council of Canada (NSERC) (SKM); SIA is grateful to Ministry of Education and Science of Russian Federation, for partial support in the frame of research project, allocated to Kazan Federal University for the state assignment in the sphere of scientific activities (#3.2166.2017/4.6). SIA is grateful to Dr. S. B. Orlinskii for high-frequency (W-band) EPR measurements at the Federal Center of Shared Facilities of Kazan Federal University.

References

1. L.-A. Liew, R.A. Saravanan, V.M. Bright, M.L. Dunn, J.W. Daily, R. Raj, Sens. Actuators A **103**, 171 (2003)
2. L.-A. Liew, W. Zhang, V.M. Bright, L. An, M.L. Dunn, R. Raj, Sens. Actuators A **89**, 64 (2001)
3. L.-A. Liew, Y. Liu, R. Luo, T. Cross, L. An, V.M. Bright, M.L. Dunn, J.W. Daily, R. Raj, Sens. Actuators A **95**, 120 (2002)
4. M. Zaheer, T. Schmalz, G. Motz, R. Kempe, Chem. Soc. Rev. **41**, 5102 (2012)
5. M. Hojamberdiev, R.M. Prasad, C. Fasel, R. Riedel, E. Ionescu, Eur. J. Ceram. Soc. **33**, 2465 (2013)
6. G. Mera, M. Gallei, S. Bernard, E. Ionescu, Nanomaterials **5**, 468 (2015)
7. S.I. Andronenko, I. Stiharu, S.K. Misra, J. Appl. Phys. **99**, 113907 (2006)
8. S.I. Andronenko, I. Stiharu, S.K. Misra, C. Lacroix, D. Menard, Appl. Magn. Reson. **38**, 385 (2010)
9. S.I. Andronenko, A. Leo, I. Stiharu, S.K. Misra, Appl. Magn. Reson. **39**, 347 (2010)
10. Alfin Leo, Sergey Andronenko, Ion Stiharu, Rama B. Bhat, Sensors **10**, 1338 (2010)
11. D.Y. Lin, C.F. Li, Y.S. Huang, Y.C. Jong, Y.F. Chen, L.C. Chen, C.K. Chen, K.H. Chen, D.M. Bhusari, Phys. Rev. B **56**, 6498 (1997)
12. A.M. Hermann, Y.T. Wang, P.A. Ramakrishnan, D. Balzar, L. An, C. Haluschka, R. Riedel, J. Am. Ceram. Soc. **84**, 2260 (2001)
13. S. Trassl, M. Puchinger, E. Rössler, G. Ziegler, J. Eur. Ceram. Soc. **23**, 781 (2003)
14. S. Trassl, G. Motz, E. Rossler, G. Ziegler, Non-Cryst. Sol. **293–295**, 261 (2001)
15. S. Trassl, G. Motz, E. Rossler, G. Ziegler, J. Am. Ceram. Soc. **85**, 239 (2002)
16. S. Trassl, H.-J. Kleebe, H. Stormer, G. Motz, E. Rossler, G. Ziegler, J. Am. Ceram. Soc. **85**, 1268 (2002)
17. E. Erdem, V. Mass, A. Gembus, A. Schulz, V. Liebau-Kunzmann, G. Fasel, R. Riedel, R.-A. Eichel, Phys. Chem. Chem. Phys. **11**, 5628 (2009)
18. F. Berger, A. Muller, F. Albinger, K. Muller, Z. Anorg, Allg. Chem. **631**, 355 (2005)
19. Y. Li, Y. Yu, H. San, Q. Han, L. An, J. Mater. Sci. Chem. Eng. **3**, 9 (2015)
20. Y.-L. Li, E. Kroke, R. Riedel, C. Fasel, C. Gervais, F. Babonneau, Appl. Organomet. Chem. **15**, 820 (2001)
21. E. Tomasella, L. Spinelle, A. Bousquet, F. Rebib, M. Dubois, C. Eypert, J.P. Gaston, J. Cellier, Plasma Process. Polym. **6**, S11–S16 (2009)
22. E. Tomasella, F. Rebib, M. Dubois, J. Cellier, M. Jacquet, J. Phys. Conf. Ser. **100**, 082045 (2008)
23. K. Kobayashi, H. Yokoyama, M. Endoh, Appl. Surf. Sci. **254**, 6222 (2008)

24. D. Savchenko, V. Kulikovsky, V. Vorliček, J. Lanček, V. Kiselov, E. Kalabukhova, Phys. Stat. Sol. B **251**, 1178 (2014)
25. E. Sawatzky, I.E.E.E. Trans. Magn. **7**, 374 (1971)
26. J. Kliava, R. Berger, J. Magn. Magn. Mater. **205**, 328 (1999)
27. T. Shimizu, M. Kumeda, Y. Kiriyama, Solid State Commun. **37**, 699 (1981)
28. N. Ishii, M. Kumeda, T. Shimizu, Jpn. J. Appl. Phys. **20**, L673 (1981)
29. S.K. Misra, Phys. Rev. B **58**, 14971 (1998)
30. A.V. Vasin, S.P. Kolesnik, A.A. Konchits, A.V. Rusavsky, V.S. Lysenko, A.N. Nazarov, Y. Ishikawa, Y. Koshka, J. Appl. Phys. **103**, 123710 (2008)
31. J.E. Wertz, J.R. Bolton, *Electron Spin Resonance: Elementary Theory and Practical Applications* (McGraw-Hill Book Company, New York, 1972)
32. A. Saha, R. Raj, D.L. Williamson, J. Am. Ceram. Soc. **89**, 2188 (2006)
33. A. Saha, R. Raj, J. Am. Ceram. Soc. **90**, 578 (2007)
34. N. Resta, C. Kohler, H.-R. Treblin, J. Am. Ceram. Soc. **86**, 1409 (2003)
35. O.E. Andersson, B.L.V. Prasad, H. Sato, T. Enoki, Y. Hishiyama, Y. Kabaragi, M. Yoshikawa, S. Bandow, Phys. Rev. B **58**, 16387 (1998)
36. B.L.V. Prasad, H. Sato, T. Enoki, Y. Hishiyama, Y. Kaburagi, A.M. Rao, P.C. Eklund, K. Oshida, M. Endo, Phys. Rev. B **62**, 11209 (2000)